10.1

PRECIPITATION OVER MULTISCALE TERRAIN

Qingfang Jiang *
Yale University, New Haven, Connecticut

1. INTRODUCTION

Although orographic precipitation has been the focus of numerous studies, little work has been done on precipitation over multiscale terrain. For example, in global scale model simulations (e.g., ECMWF) or idealized studies (e.g., Schneidereit and Schär, 2000), the Alps was often treated as an about 300km long and 150km wide smooth ridge. The resolution of observational network is usually too coarse to resolve small scale features ($< 20km$). For example, the resolution of the climatological precipitation field derived from raingauge data by Frei and Schär (1998) was 25km. However, some case studies (Bruintjes, 1994; Smith et al 2002) indicated strong spatial variation of precipitation patterns which were closely tied to individual peaks with horizontal dimensions of 20km or less.

In this idealized study, moist airflow over a pair of two-dimensional Gaussian shaped hills are examined using a mesoscale model (Atmospheric Regional Prediction System, or ARPS, Xue et al, 1995) with explicit cloud parameterization (Lin et al, 1983). The focus of this study is the variation of windward lift and precipitation efficiency with mountain scales.

2. NUMERICAL SETUP

The topography is a pair of 2-D Gaussian type mountain specified by (Fig 1)

$$h(x) = h_m exp(-(x - x_0 + b/2)^2/a^2) + h_m exp(-(x - x_0 - b/2)^2/a^2) \quad (1)$$

where h_m is the maximum mountain height, a is the mountain half width, x_0 is the location of the terrain, and b is the distance between the two peaks. The model grids are 503×41 and the spatial grid sizes are $DX = 2000m$ and $Dz = 500m$. A terrain-following coordinate is used and the vertical coordinate is further stretched using a cubic function with $\delta z_{min} = 100m$ between the lowest two layers. At $z_{top} = 12000m$, the terrain-following coordinate surfaces becomes flat.

* Corresponding author address: Qingfang Jiang, Yale University, Dept. of Geology, New Haven, CT06520-8109; email: qingfang.jiang@yale.edu

The model is initialized using a single sounding. The temperature profile is specified with a constant surface temperature T_0 and two constant buoyancy frequency for dry air(N_d) to represent the less stable ($N_d = 0.012s^{-1}$) troposphere and more stable $N_d = 0.025s^{-1}$ stratosphere. The wind is from left to right with a uniform speed of $U_0 = 20m/s$. The relative humidity is 92% in the troposphere and 40% in the stratosphere.

Some fields from the solution with a=20km, $h_m = 800m$, and b=80km are shown in Fig. 1. There is weak blocking upstream of the first peak and strong downslope wind ($\sim 28m/s$) over leesides of both peaks (Fig 1a). The large vertical wavelength and nearly vertical phase line indicate that the moist low level flow is weakly stable. Figure 1b shows the the vertical motion is stronger upslope of the second peak. Figure 1c shows that rain water is generated over the first peak, the second peak, and in the lee waves downstream of the second peak. The rain water reaches maximum right over the first peak.

3. WINDWARD ASCENT

For the purpose of diagnosis, we define W(x), the vertical speed averaged over the lower troposphere, as an index of terrain windward lift effect,

$$W(x) = \int_0^H w(x,z)dz/H_0 \quad (2)$$

where w(x,z) is integrated from the ground to either where w(x,z) is less than an arbitrary threshold (0.0001m/s) or to $H_0 = 4km$ whichever condition is met first. Therefore, W(x) is always positive and waves aloft do not contribute to W(x). Figure 2 indicates that windward lift over the first peak is insensitive to b, the inter-mountain distance. The lift over the second peak is very sensitive to b. For b=40km, W(x) over the up-wind slope of the second peak is about a half of that of the first peak, and for b=80km, it is about 40% more than that of the first peak.

For a single wide mountain, the windward lift is much weaker and more widespread (Fig 3). Figure 4 shows the lift by a mountain of 800m high and 100km wide. The maximum of W(x) induced by a 800m high and 100km wide mountain is about

20% of the maximum W(x) induced by the first peak of the narrow (a=20km) twin mountains in Fig 3, which roughly agrees with the scaling $w \propto Uh_m/a$.

4. PRECIPITATION EFFICIENCY

Figure 3 shows that location and rate of precipitation over the first peak are insensitive to b, the inter-mountain distance. The precipitation pattern shifts about 20km downstream of the lift pattern. The precipitation rates over the second peak are much weaker for both b values. Especially for b=80km, W(x) over the second peak is about 40% more than that over the first peak. The corresponding precipitation rate is only 80% of its corresponding value over the first peak, however. If we define precipitation efficiency (PE) for a cloud as the area integrated precipitation rate over the volume (of the cloud) integrated condensation rate (Jiang and Smith, 2002), the PE is about 35% over the first peak is and about 20% over the second peak. According to Jiang and Smith (2002), precipitation efficiency for a cloud dominated by nonlinear accretion growth of hydrometeors is

$$PE = \frac{1 - 1/R}{1 + \tau_f/\tau_a} \tag{3}$$

where where $\tau_a = a/U$ is advection timescale, τ_f is the time it takes for hydrometeors to fall to the ground, and R is the nondimenional condensation rate which is proportional to the incoming moisture flux. A fair portion of water vapor is drained out by the first peak so that the water vapor flux that hits the second peak is much reduced (Fig 1d). The R for the cloud over the second peak is much smaller, and so is the PE according to equation (3).

Precipitation over a single wide mountain is weaker and more wide spread (Fig 3). The precipitation efficiency for the mountain of a=100km is about twice the PE of the first peak of the twin narrow mountains. The increase of PE with mountain width is interpreted by Jiang and Smith (2002) using the following equation

$$PE = \frac{1}{(1 + \tau_r/\tau_a)(1 + \tau_f/\tau_a)} \tag{4}$$

where τ_r is the conversion time form condensed water to a type of precipitable hydrometeor. Equation (4) assumes linear growth of hydrometeors. As an example, if we choose $\tau_r = \tau_f = 1000sec$, we have PE = 25% for a=20km and PE = 70% for a = 100km.

5. CONCLUSIONS

This study suggests that the precipitation efficiency can be significantly increased as multiscale terrain with small scale peaks being replaced by a large smooth terrain. For multiscale terrain, the advection timescale that decides precipitation efficiency seems related to the dimensions of individual peaks. The first peak is much more efficient in draining water out of the atmosphere due to nonlinear processes.

6. ACKNOWLEDGMENTS

The author thanks Dr. Ronald Smith for his constructive comments and suggestions. This research was supported by the National Science Foundation, Division of Atmospheric Sciences (ATM-9711076). The simulations were made using the Advanced Regional Prediction (ARPS) developed by the Center for Analysis and Prediction of Storms (CAPS), University of Oklahoma. CAPS is supported by the National Science Foundation and the Federal Aviation Administration.

7. REFERENCE

Bruitjes, R. T., 1994: Interactions between Topographic Airflow and Cloud/Precipitation Development during the Passage of a Winter Storm in Arizona. *J. Atmos. Sci.*, **51**, 48-67.

Frei, C. and Schär, 1998: A precipitation climatology of the Alps from high resolution rain-gauge observations. *Int. J. Climatol.*, **18**(9): 873-900.

Jiang and Smith, 2002: Cloud timescale and orographic precipitation. submitted to *J. Atmos. Sci.*.

Kessler, E., 1969: On the distribution and continuity of water substance in atmospheric circulations. *Meteor. Monogr.*, **32**, Amer. Meteor. Sco., 84pp.

Lin, Y. L., R. D. Farley, and H. D. Orville, 1983: Bulk parameterization of the snow field in a cloud model. *J. Clim. Appl. Meteor.*, **22**, 1065-1092.

Schneidereit, M. and C. Schär, 2000: Idealised Numerical Experiments of Alpine Flow Regimes and Southside Precipitation Events. *Meteorol. Atmos. Phys.*, **72**, 233-250.

Schultz, P., 1995: An explicit cloud physics parameterization for operational numerical weather prediction. *Mon. Wea. Rev.*, **123**, 3331-3343.

Smith et al, 2002: Orographic precipitation and airmass transformation: An Alpine example. submitted to *Quart. J. R. Meteor. Soc.*.

Xue, M., K. K. Droegemeier and V. Wong The Advanced Regional Prediction System (ARPS) - a multiscale nonhydrostatic atmospheric simulation and prediction tool. Part I: Model dynamics and verification. *Meteorol. Atmos. Physics*, **75**, 161-193.

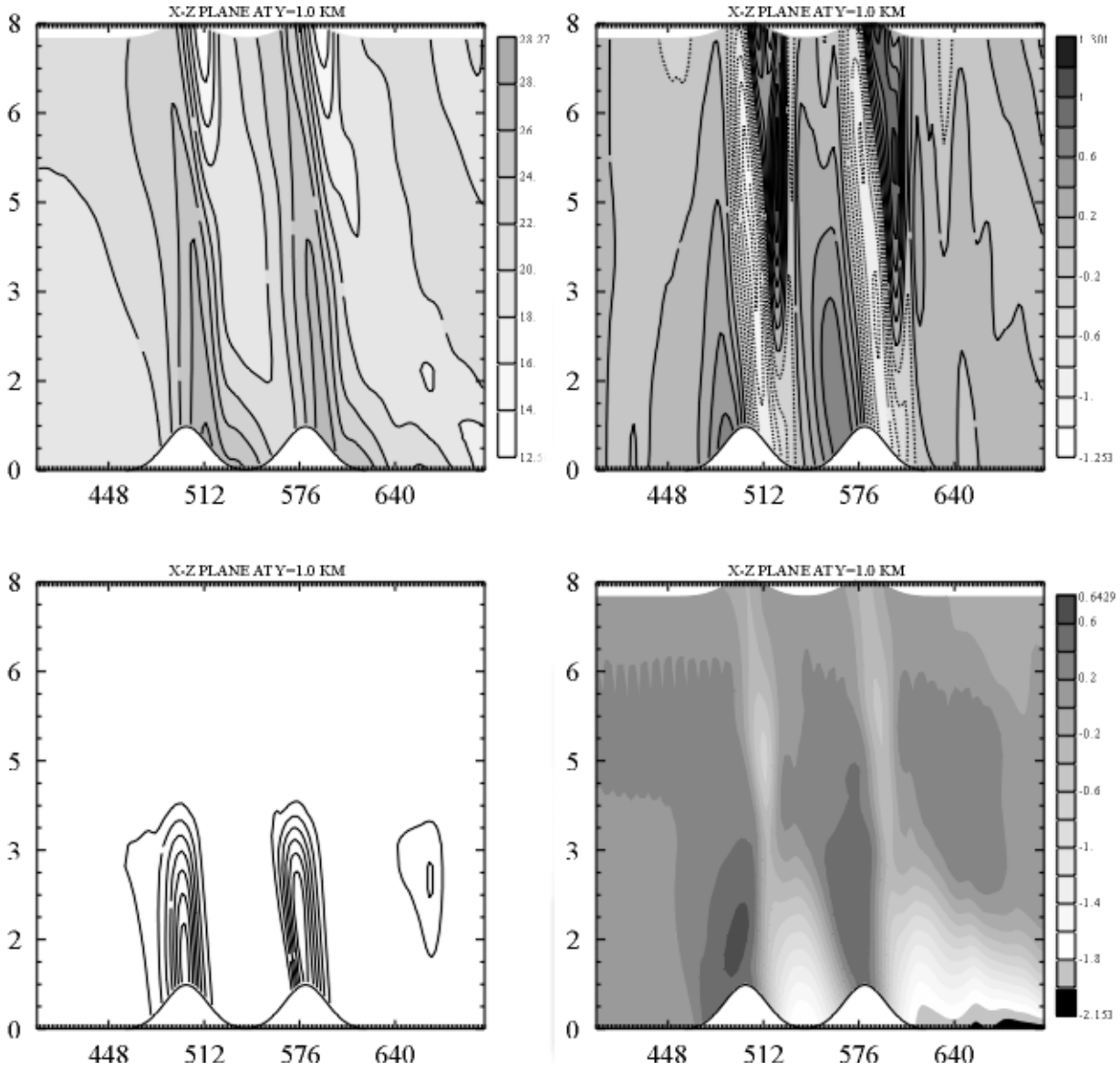

Figure 1: Vertical cross section at T =2 hours with $h_m = 800m$, $a = 20km$, and $b = 80km$. a) u-component of wind; b) w-component of wind; c) mixing ratio of rain water; d) perturbation of water vapor mixing ratio. Only a portion of the domain is plotted.

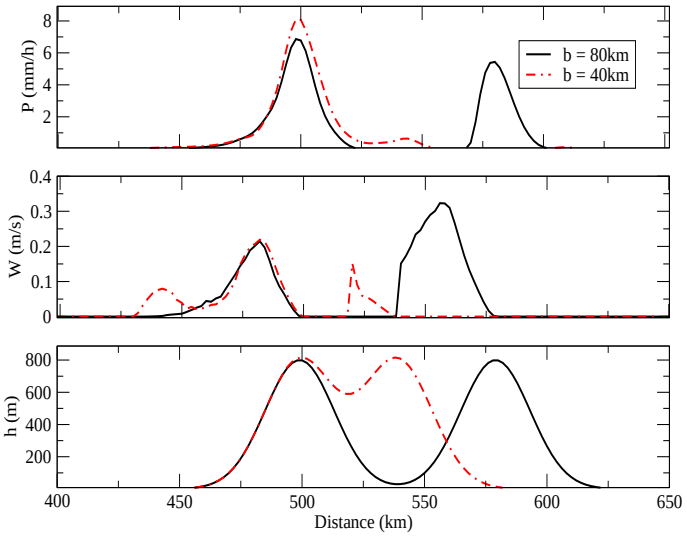

Figure 2: Precipitation and lift versus along wind distance for two runs with $h_m = 800m$, a=20km, and b=40km, 80km. a) Precipitation rate, b) windward lift (W(x)), c) terrain (h(x)).

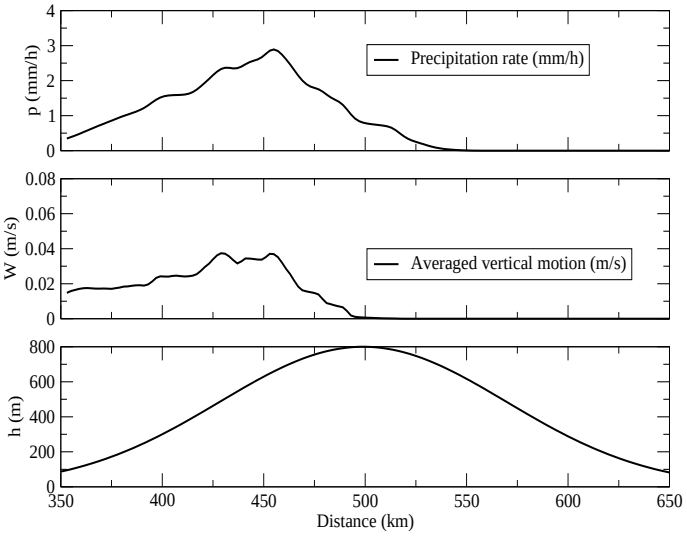

Figure 3: Same as Fig 2 but for a single mountain of a=100km

.